

Application Data

Endless possibilities

Light changes the world.



Functional Materials



ELSZ-2000

Zeta-potential & Particle size Analyzer



DLS-8000 SLS-6500

Dynamic Light Scattering Spectrophotometer



Agilent 7100

Capillary Electrophoresis

Otsuka Electronics Co.,Ltd.

Otsuka Electronics Co.,Ltd.

6F Eslead Bldg.
Otedori, Chuo-ku. Osaka, 540-0021, Japan
Tel : +81-6-6910-6521
Fax : +81-6-6910-6528



<http://www.otsukael.jp/>

INDEX



ELSZ

Zeta-potential & Particle size Analyzer ELSZ-2000



DLS / SLS

Dynamic Light Scattering Spectrophotometer DLS-8000 / SLS-6500



CE

Capillary Electrophoresis Agilent 7100

Nanocarbon materials

Fullerene	ELSZ	P.04	1	Particle diameter evaluation of fullerenes	Particle diameter	
Carbon nanotube	ELSZ	P.04	2	Evaluation of the distribution of carbon nanotubes when exposed to an anionic surfactant	Particle diameter	
	DLS	P.05	3	Evaluating the axial ratio of carbon nanotubes by depolarized dynamic light scattering	Theory	Particle diameter
	DLS	P.05	3		Measurement	Particle diameter
	ELSZ	P.06	4	Dispersion evaluation of carbon nanotubes with various dispersants	Zeta potential	
Carbon nanohorn	ELSZ	P.06	5	Evaluating porosity of carbon nanohorns	Particle diameter	Zeta potential

Colloid particles

Inorganic particles	ELSZ	P.07	6	Evaluating the particle diameter and zeta potential of colloidal gold particles	Particle diameter	Zeta potential
	ELSZ	P.07	7	Particle diameter evaluation of quantum dots	Particle diameter	
	ELSZ	P.08	8	Evaluating isoelectric points of inorganic particles by pH variation	Zeta potential	
	ELSZ	P.08	9	Identifying optimal additive concentrations	Particle diameter	Zeta potential
	ELSZ	P.09	10	Evaluating flocculants used in water treatment	Particle diameter	Zeta potential
	ELSZ	P.09	11	Evaluating the effectiveness of adding nonionic surfactant to control zeta potential and particle diameter for CMP slurry	Particle diameter	Zeta potential

Surfactant micelle	ELSZ	P.10	12	Particle diameter evaluation of surfactant micelles in pure water	Particle diameter
	ELSZ	P.10	13	Particle diameter evaluation of surfactant micelles with and without salt present	Particle diameter
	ELSZ	P.11	14	Evaluating aggregation numbers of surfactant micelles by static light scattering	Molecular weight

Polymer

Synthetic polymer	ELSZ	P.12	15	Evaluating the properties of an electroconductive polymer (PEDOT/PSS)	Particle diameter	
	ELSZ	P.12	16	Evaluating the alternate lamination method based on solid surface potential	Zeta potential	
	ELSZ	P.13	17	Temperature gradient evaluation of polystyrene in cyclohexane	Particle diameter	
	SLS	P.13	18	Evaluating the characteristics of functional polymers by static light scattering	Molecular weight	
	ELSZ	P.14	19	Zeta potential evaluation for plastic containers	Zeta potential	
	CE	P.14	20	Quantitative evaluation of impurities in terephthalic acid	Separation analysis	
Natural polymer	ELSZ	P.15	21	Evaluating casein at normal and low temperatures	Zeta potential	
	ELSZ	P.15	22	Evaluating fibrous and filamentous samples	Particle diameter	Zeta potential
	ELSZ	P.16	23	Evaluating zeta potential in the fiber dyeing process	Zeta potential	
	ELSZ	P.16	24	Evaluating printer paper surfaces	Zeta potential	

1

ELSZ Particle diameter evaluation of fullerenes

Particle diameter

Purpose Nanocarbon are substances consisting of carbon particles measuring no more than 100 nm in diameter. Fullerenes, carbon nanotubes (CNTs), graphenes, and carbon nanocapsules are nanocarbons. Due to their intrinsic mechanical properties, thermal conductivity properties, and electrical conductivity properties, these materials have applications in various fields ranging from electronics to biological research to medical care.

In our study, we measured the particle diameter of a fullerene (C₆₀) consisting of 60 carbon atoms.

Result Figure 1 shows the distribution of particle diameters of fullerene (C₆₀). We see a peak at 0.7 nm.

The results are consistent with the size of the fullerene structure shown in Figure 2.

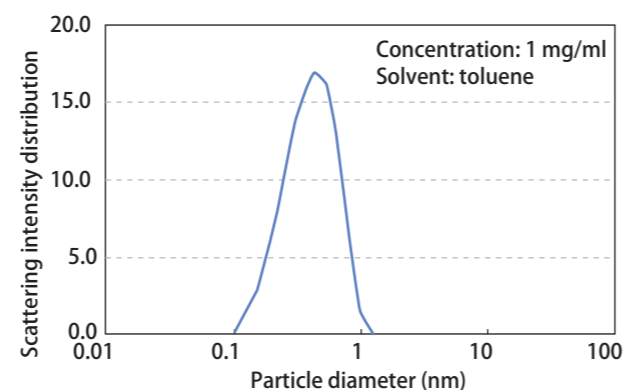


Fig. 1 Distribution of particle diameters of fullerene (C₆₀)

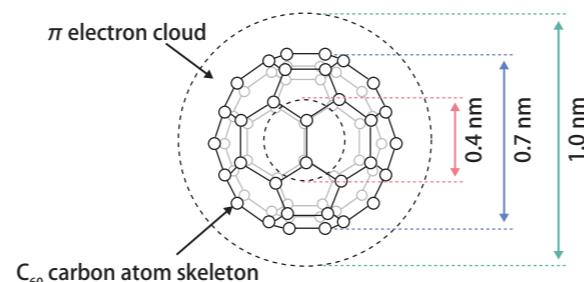


Fig. 2 Structure of fullerene (C₆₀)

2

ELSZ Evaluation of the distribution of carbon nanotubes when exposed to an anionic surfactant

Particle diameter

Purpose Carbon nanotubes (CNT) are used as materials in the fields of electronics and fuel cells. To optimize the intrinsic electrical and mechanical properties of CNTs, a key first step is dispersion that loosens the aggregation state.

We evaluated the dispersibility of CNT with respect to particle diameter and zeta potential using sodium dodecyl-sulfate (SDS), an anionic surfactant, as the dispersant.

Result Figure 1 and Table 1 present measurement results for the particle diameter and zeta potential of the CNTs with SDS present and absent. SDS reduced the particle diameter of the CNTs from 959.6 nm to 245.3 nm. Adding SDS also narrowed the distribution of particle diameter.

With respect to zeta potential, adding SDS increased negative charge. This means we can evaluate distribution states based on particle diameter and that zeta potential is an index of electrostatic repulsion, which governs dispersibility.

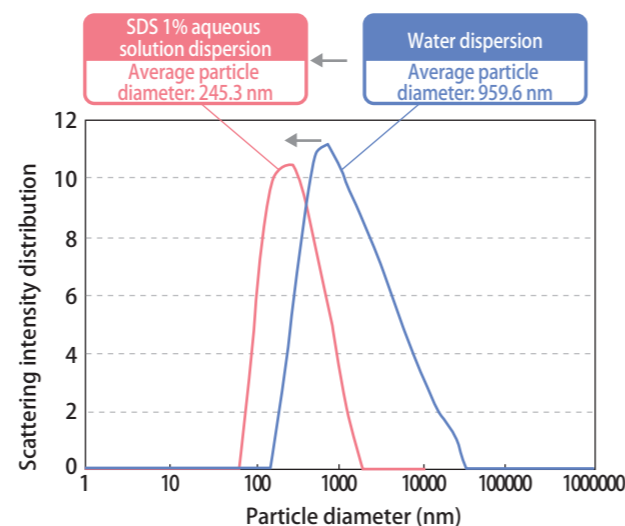


Fig. 1 Particle distribution of CNTs with SDS present/absent

Table 1 Average particle diameter and zeta potential of CNTs with SDS present/absent

SDS	Average particle diameter (nm)	Zeta potential (mV)
Absence	959.6	-43.8
Presence	245.3	-69.9

3

DLS Measuring the axial ratio of carbon nanotubes by depolarized dynamic light scattering

Particle diameter

Theory When a sample is irradiated by vertically polarized incident light, polarized scattering, I_{VV} , is given by a light passing through a vertically oriented polarizer. Scattered light obtained with a horizontally oriented polarizer is called depolarized scattering and expressed by I_{HV} . While polarized scattering depends mainly on the translational motion of particles, depolarized scattering derives from the optical anisotropy of particles in the scattering medium.

If the particles are spherical, depolarized scattering equals zero. If the particles like rod-like particles rotate, the intensity of the depolarized component varies with movement. The measurement provides information on the rotation of optically anisotropic particles.

When we measure dynamic light scattering with polarizer oriented horizontally in front of the detector, we obtain information concerning rotation of particles (rotational diffusion coefficient).

Equation (1) gives the correlation function.

$$\langle I_{HV}(0)I_{HV}(t) \rangle = Be^{-\Gamma t} = Be^{-\Gamma} = Be^{-(q^2Dt + 6Dr)t} \dots (1)$$

Here, D_t represents the translational diffusion coefficient, D_r the rotational diffusion coefficient, and $q (= 4\pi n \sin(\theta/2)/\lambda)$ the scattering vector.

If we plot Γ (decay constant obtained by measuring dynamic light scattering of depolarized scattering by varying angle of measurement and plotted) on the vertical axis against q^2 on the horizontal axis as shown in figure 1, we obtain $1/6$ of the intercept as D_r . The slope is D_t .

We can calculate the lengths of the long axis (L) and short axis (d) from D_t and D_r using the Kirkwood-Riseman¹⁾ relation expressed by equation (2).

The axial ratio (aspect ratio) is given by L/d .

$$\begin{aligned} D_t &= 3kT \times \ln(L/d) / \pi \eta L^3 \dots \dots \dots (2) \\ D_r &= kT \times \ln(L/d) / 3\pi \eta L \end{aligned}$$

Here, T : absolute temperature, k : Boltzmann's constant, η : viscosity of medium

Measurement In addition to information on translational motion, depolarized dynamic light scattering provides information concerning the rotation of anisotropic particles (rod-like particles), or the rotational diffusion coefficient. Using the rotational diffusion coefficient obtained and the translational diffusion coefficient, we can obtain the lengths of the long axis (L) and short axis (d) based on the Kirkwood-Riseman equation and calculate the axial ratio (aspect ratio).

We dispersed multi-walled carbon nanotubes (Aldrich: length 0.5 to 2.0 μm , outer diameter 20 to 30 nm, inner diameter 1 to 2 nm) in a 1% aqueous sodium dodecyl sulfate solution at a concentration of 0.002 wt% and performed depolarized dynamic light scattering measurements. Since the results obtained were within the range of assumed values, we assumed the axial ratio obtained is an appropriate result. Although improvement of condition of dispersion of the sample is essential, depolarized dynamic light scattering method is capable of obtaining axial ratio of rod-like particles and is expected to provide valuable information.

Table 1 Carbon nanotube measurement results obtained by depolarized dynamic light scattering

Translational diffusion coefficient (cm^2s^{-1})	Rotational diffusion coefficient (s^{-1})	Long axis (nm)	Short axis (nm)	Axial ratio
2.6×10^{-8}	5.5×10^1	653.4	21.26	30.7

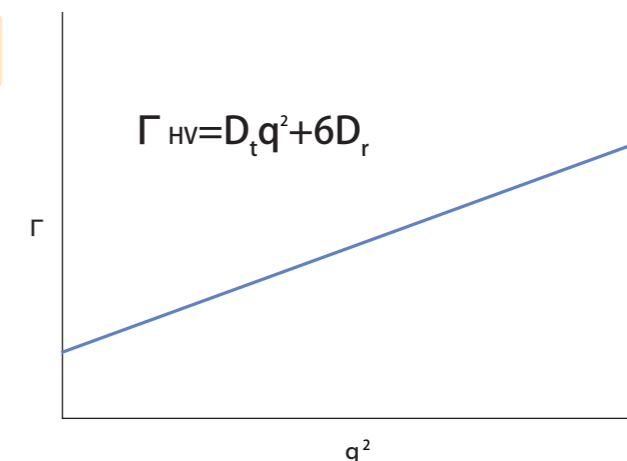


Fig. 1 Plot for obtaining rotational scattering coefficient and translational scattering coefficient

<Reference>

1) J. Riseman and J. Kirkwood: J.Chem.Phys., 18(4), 512-516 (1950)

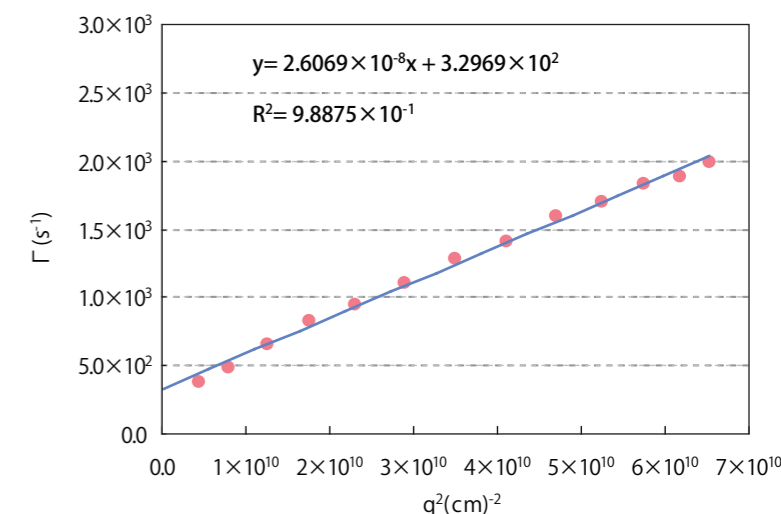


Fig. 2 Plot for obtaining rotational diffusion and translational diffusion coefficients for carbon nanotubes

4

ELSZ

Dispersion evaluation of carbon nanotubes with various dispersants

Zeta potential

Purpose Carbon nanotubes, a key material of high interest in the field of nanotechnology, resist dispersion in water and organic solvents. The question of how to disperse CNTs in solvents has emerged as a major issue.

We added commercially available multi-walled carbon nanotubes at a concentration of 0.002 wt% to each of several 1% aqueous solutions: an inorganic dispersant, sodium hexametaphosphate (HMPNa) and nonionic surfactants, sodium dodecyl sulfate (SDS) and sodium dodecyl benzene sulfonate (NaDDBS). Following dispersion by ultrasonication for 5 minutes, we measured the zeta potential to evaluate dispersion effects.

Result Figure 1 shows results for zeta potential evaluations.

The absolute value of the zeta potential was greater, corresponding to better dispersant, for surfactants than for inorganic electrolytes.

We conclude that zeta potential measurement is an effective method that allows ready evaluation of dispersant effects.

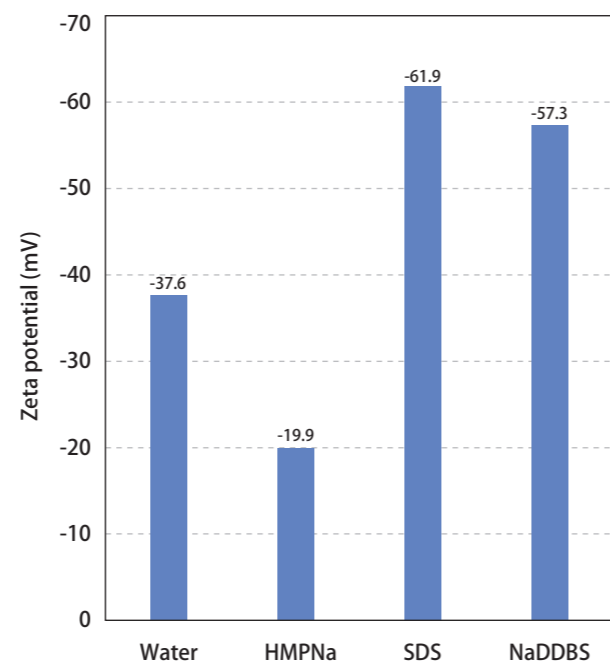


Fig. 1 Zeta potential of carbon nanotubes with different dispersants

5

ELSZ

Evaluating porosity of carbon nanohorns

Particle diameter

Zeta potential

Purpose Carbon nanohorns (CNHs), a type of nanocarbon, are conical graphenes. Producing CNHs is easier than CNTs, and the mass production of CNHs is also fairly easy. Since CNHs can be made porous to serve as a substance carrier, they are attractive candidates for drug delivery and other applications.

We measured the particle diameter and zeta potential of CNHs with and without pores.

Result Figure 1 and Table 1 give the particle diameters and the zeta potential of CNHs with and without pores. Measurement of particle diameters indicate the presence of aggregates for CNHs without pores. Zeta potential measurements of CNHs showed negative charge. Porous CNHs in particular showed large negative values. The greater negative charge is believed to be attributable to modifying porous CNH with anionic dissociable groups.

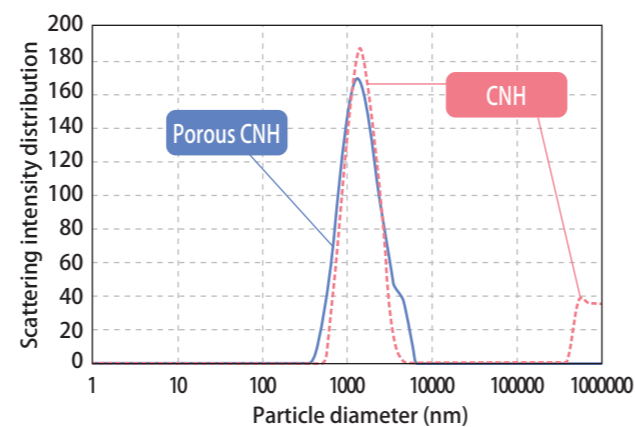


Fig. 1 Distribution of particle diameters of CNHs with and without pores

Source of samples: NEC Corporation

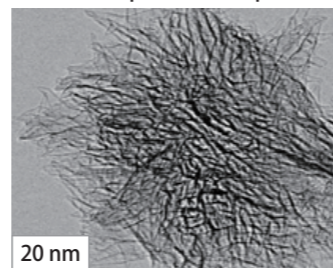


Table 1 Average particle diameter and zeta potential of CNHs with and without pores

	Average particle diameter (nm)	Zeta potential (mV)
CNH	1433 nm	-9.4 mV
Porous CNH	1449 nm	-20.0 mV

6

ELSZ

Evaluating the particle diameter and zeta potential of colloidal gold particles

Particle diameter

Zeta potential

Purpose Known to change color as it interacts with visible light, colloidal gold has been used from antiquity to color glass and pottery. In recent years, it has been used in fields related to diagnostics, pharmaceuticals, biomarkers, markers for X-ray analysis, and other applications in high-tech areas like organic solar cells and catalysts.

We measured the particle diameter and electrical mobility of commercially available colloidal gold characterized by different particle diameters.

Result Figure 1 shows the results of particle diameter measurements of colloidal gold ranging from 2 nm to 50 nm by dynamic light scattering. The measured particle diameters were in near perfect agreement with indicated values for all colloidal gold, demonstrating the efficacy of dynamic light scattering.

Measurements of the electrophoretic mobility of colloidal gold of different particle diameters give results of -4×10^{-4} (cm^2/Vs) for all particle sizes of colloidal gold. This is due to the same compositions showing that production methods are the same.

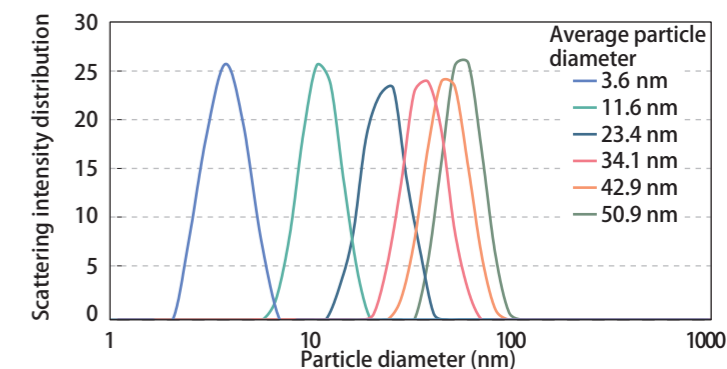


Fig. 1 Particle size distribution of colloidal gold of different particle diameters

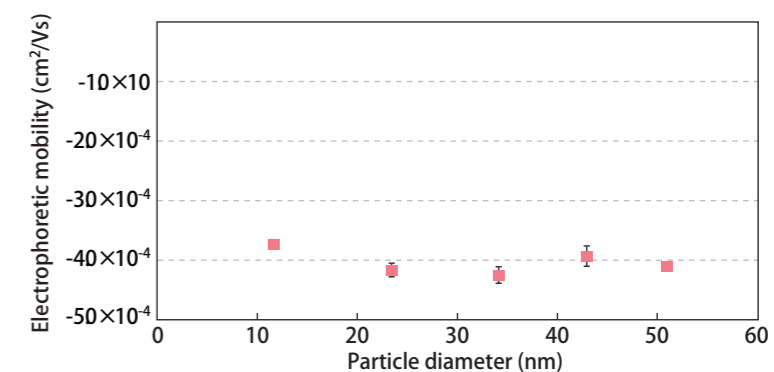


Fig. 2 Electrophoretic mobility of colloidal gold of varying particle diameters

7

ELSZ

Particle diameter evaluation of quantum dots

Particle diameter

Purpose Quantum dots are nanoscale semiconductor particles ranging from 2 to 20 nm. As their characteristics, they are capable of absorption and changing luminescent color of arbitrary light by controlling particle size, and light of any wave length may be efficiently utilized because of high luminous efficiency. Because of their characteristics, usage in lighting, display, solar cells, biological imaging, etc., is expected. Since properties of quantum dots vary depending on control of particle size, particle diameter control and dispersion technology are important.

We measured the particle diameters of commercially available quantum dots.

Result Figures 1 and 2 show measurement results for QD490 nm and QD575 nm.

The average particle diameters for QD490 nm and QD575 nm, respectively, were 7.2 nm and 8.3 nm. Both distributions showed a single peak. There are quantum dots of core-shell type, core-shell type with surface modification groups, etc. Particle diameters of quantum dots including shells and surface modification groups are measured by dynamic light scattering.

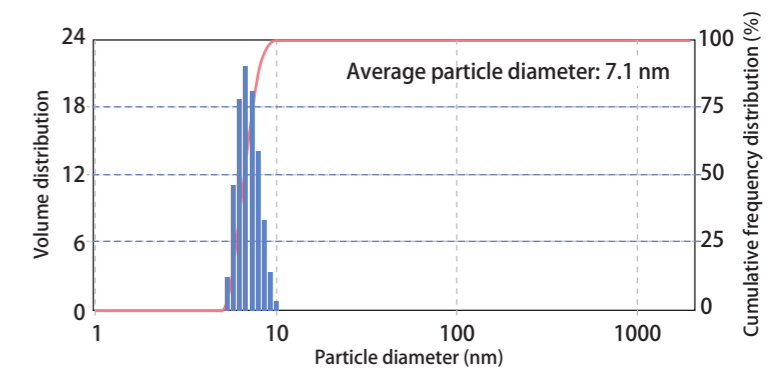


Fig. 1 Particle size distribution of QD490 nm

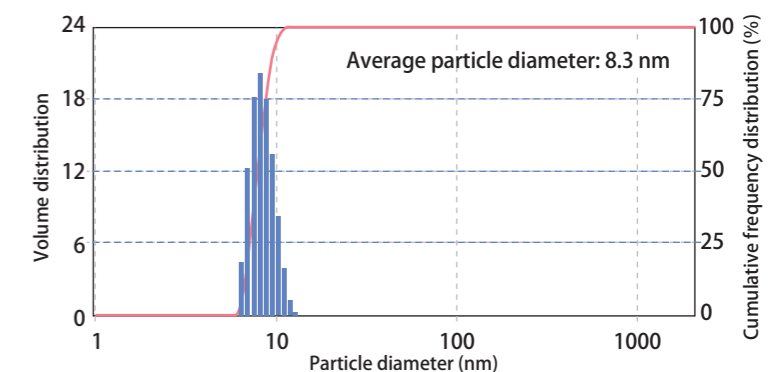


Fig. 2 Particle size distribution of QD575 nm

Evaluating isoelectric points of inorganic particles by pH variation

Purpose Many colloid dispersion systems change their characteristics depending on pH. pH titration measurements can bring to light various characteristics of materials not obtained under unvarying measurement conditions. Essential to pursuing highly reproducible process control, this method has wide applications involving inorganic powders, ceramics, sewage treatment, cleaning, fibers, chemistry, biology, and food.

We performed pH titration of commercially available alumina (Al_2O_3), silica (SiO_2), titanium oxide (TiO_2), and a compound of alumina and silica ($3\text{Al}_2\text{O}_3 \cdot 2\text{SiO}_2$) using a pH titrator and determined isoelectric points.

Result Figure 1 shows the results from the pH titration of each particle. The isoelectric points determined for the inorganic oxides were $\text{pI} = 9.6$ for alumina, $\text{pI} = \text{less than } 3$ for silica, and $\text{pI} = 5.6$ for titanium oxide. Isoelectric points can vary depending on crystal structures, but the values are almost the same as those in literature.

Isoelectric point of compound of alumina and silica, $3\text{Al}_2\text{O}_3 \cdot 2\text{SiO}_2$, is $\text{pI} = 7.4$, in acid side compared with that of alumina. This is considered to be influenced by silica.

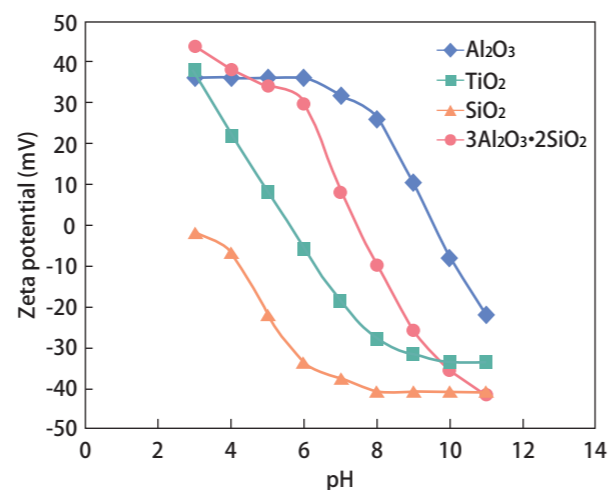


Fig. 1 Results for pH titration of each inorganic compound

Identifying optimal dispersant concentrations

Purpose The dispersion stability of colloid particles is a key issue in many industries, and related research and applications are promoted. Particle diameter, zeta potential are used as indices of dispersion stability.

We investigated optimal dispersion concentrations using alumina particles and sodium metaphosphate (HMPNa), an inorganic dispersant. We varied the concentrations of the dispersant added and tracked changes in particle diameter and zeta potential over time following the addition of the dispersant.

Result Figures 1 and 2 show results for the measurement of particle diameter and zeta potential of alumina particles 2, 30, and 60 minutes after adding dispersant of various concentrations. The particle diameters varied with differing concentrations ranging from 1×10^{-2} mM to 5×10^{-2} mM; they also varied over time.

We identified a major difference at a concentration of 3×10^{-2} mM, at which particle diameters grew about eventually tripled over time. The zeta potential is close to zero near this concentration. The instability of dispersion system due to the adsorption of HMPNa is considered to appear in the concentration range where inversion from positive charge to negative charge occurs.

The results suggest the optimal concentration of HMPNa is 1×10^{-2} mM, at which particle diameters are small and the absolute value of zeta potential is large. No changes in zeta potential occurred over time. The adsorption of the dispersant occurred rapidly, within 2 minutes.

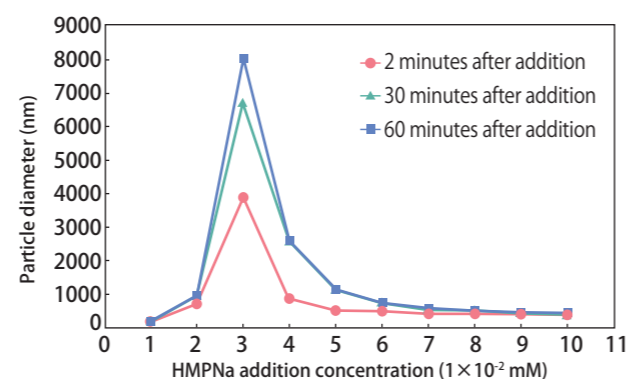


Fig. 1 Dependence of particle diameter of alumina particles on HMPNa concentrations

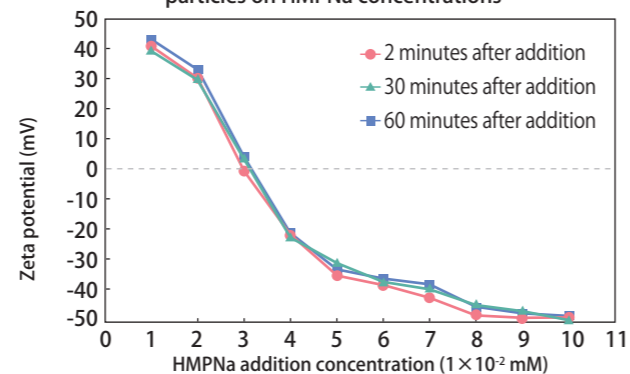


Fig. 2 Dependence of zeta potential of alumina particles on HMPNa concentrations

Evaluating flocculants used in water treatment

Purpose Mud, organic matters, microbes, and other particles are carried suspended in river water. Water treatment refers to the process of removing such impurities and suspended matter to make water potable. The treatment includes steps to flocculate and precipitate the suspended matter, after which the supernatant water is treated by filtration. Depending on the water treated, flocculants include inorganic-based and polymer-based matter.

We measured particle diameters and zeta potential to evaluate dispersion states using sodium polystyrene sulfonate (PSSNa), an anionic polymer electrolyte, as the polymer-based flocculant and alumina particles as suspended particles. We used 1 mM NaCl (pH6) as the solvent. We used an ultrasonicator for 10 minutes to achieve dispersion.

Result Since the isoelectric point is pH9 to 10, the alumina particles are positively charged at pH6. Adding PSSNa reduces the zeta potential of the alumina particles; this approaches zero at a concentration of 2.5×10^{-4} mM. Increasing concentrations still further increases the negative charge. The zeta potential of alumina became constant at around -40 mV at a concentration of 20×10^{-4} mM, indicating that PSSNa is adsorbed to the alumina particles. Adding PSSNa of lower concentrations gradually increases alumina particle diameter, leading to flocculation. Particle diameter reaches a maximum at the concentration at which zeta potential becomes zero. Further addition results in a stable concentration of 10×10^{-4} mM due to smaller particle diameters and redispersion. The results for particle diameter and zeta potential indicate the optimal concentration for flocculation is 2.5×10^{-4} mM.

In conclusion, particle diameter and zeta potential are useful indices for evaluating the effects and optimal concentration of flocculants.

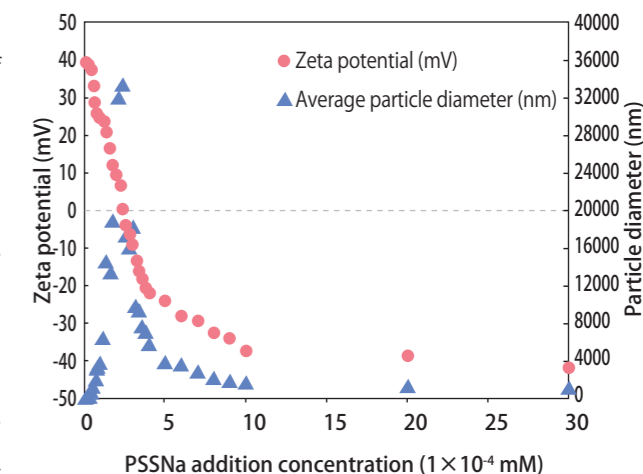


Fig. 1 Dependence of alumina particle diameter and zeta potential on PSSNa concentrations

Evaluating the effectiveness of adding nonionic surfactant to control zeta potential and particle diameter for CMP slurry

Purpose In semiconductor production CMP (chemical mechanical polishing), metal oxides (silica particles, alumina particles) are often used to polish semiconductor wafers and metal surfaces. Since various factors (e.g., pH, additives) affect the dispersion states of particles of metal oxides such as alumina particles and silica particles, controlling dispersion states with particle diameter and zeta potential as indices is an area of high interest.

We added a nonionic surfactant to CMP slurry and measured changes in zeta potential and particle diameter before and after the addition.

Result Figure 1 shows the particle size distributions before and after the addition of the nonionic surfactant. Also shown are particle diameters and zeta potentials. Without the additive, the average particle diameter was 104.2 nm and the zeta potential -34.3 mV. With the additive, the average particle diameter was 164.0 nm and the zeta potential -14.7 mV. The additive clearly affects particle diameter and zeta potential, indicating that the nonionic surfactant is adsorbed to particle surfaces, increasing particle diameters in accordance with numbers of adsorption layers.

The adsorption of the nonionic surfactant appears to lower zeta potential. Measurements of zeta potential and particle diameter allow evaluations of dispersion, offering an extremely important tool for the control of dispersion states.

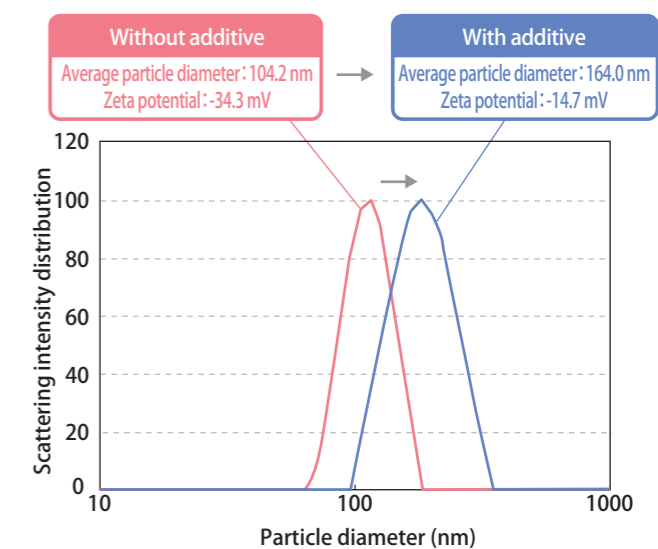


Fig. 1 Particle size distributions in CMP slurry before and after addition of nonionic surfactant

12

ELSZ

Particle diameter evaluation of surfactant micelles in pure water

Particle diameter

Purpose *Surfactant* is a collective term for substances with hydrophilic and hydrophobic groups. Such substances are also known as amphiphilic substances. When we dissolve a surfactant in water, the hydrophobic groups are surrounded by water molecules and become unstable above certain concentrations. Seeking stability, the surfactant molecules gather in flocs, forming micelles with hydrophilic groups oriented outward and hydrophobic groups oriented inward (Figure 1). This state is known as the critical micelle concentration (CMC).

We measured particle diameters of micelles of sodium dodecyl sulfate (SDS) and the nonionic surfactant Tween 20 in pure water.

Result Figure 2 shows measurement results for SDS and Tween 20 in pure water.

The particle diameters of SDS and Tween 20 were 1.1 nm and 7.6 nm. Since the molecular weights of SDS and Tween 20 are 288 and 1228, the greater the molecular weight, the larger the particle diameter of the micelle.

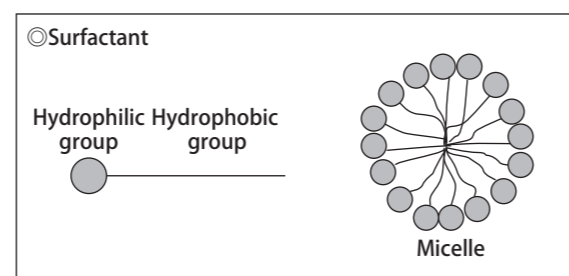


Fig. 1 Structural formula of surfactant micelles

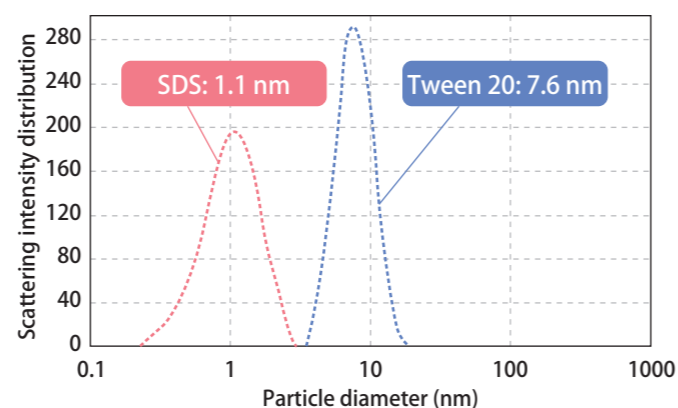


Fig. 2 Distribution of particle diameters of surfactant micelles in pure water.

13

ELSZ

Particle diameter evaluation of surfactant micelles with and without salt present

Particle diameter

Purpose Aggregation numbers of surfactant micelles vary depending on concentrations of salt in the solvent and the type of salt.

We used sodium dodecyl sulfate (SDS) as a surfactant for evaluating the state of micelle aggregation depending on salt concentration based on particle diameter measurements. We used 10 mM phosphoric acid buffer solution (pH7) as the solvent; as the salt, we used sodium chloride (NaCl).

Result Figure 1 shows results for particle diameter measurements of SDS micelles with and without NaCl present.

The particle diameter of SDS micelles in a 0 mM NaCl solution was 3.3 nm. Particle diameter increases compared to pure water due to salt concentrations in the phosphoric acid buffer solution. The particle diameter became 4.6 nm in a 100 mM NaCl solution. Greater salt concentrations result in larger particle diameters.

This indicates a higher aggregation number of micelles.

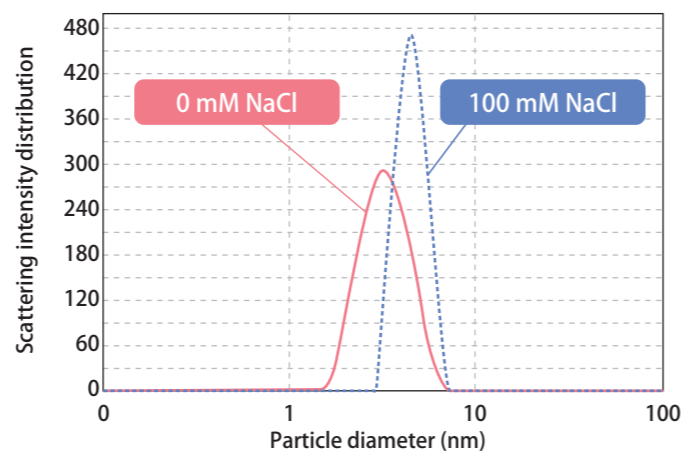


Fig. 1 Distribution of particle diameters of SDS micelles with and without NaCl

14

ELSZ

Evaluating aggregation numbers of surfactant micelles by static light scattering

Molecular weight

Purpose Surfactants form micelles, which have significant effects on cleaning and emulsification/dispersion. This makes determining the physical property values of the surfactant micelles particularly important.

We measured the molecular weight of micelles of Tween 20, a nonionic surfactant, by static light scattering and determined the aggregation number.

Result Figure 1 shows results for an analysis of a Debye plot for Tween 20.

The molecular weight of the micelle was 56110. The aggregation number of the micelle can be obtained by dividing the molecular weight of the micelle by the molecular weight of the monomer. The result was 45.

In addition to molecular weight, we can determine the second virial coefficient, which shows an affinity for the solvent, by static light scattering. The coefficient was positive. We found this to be a good solvent system.

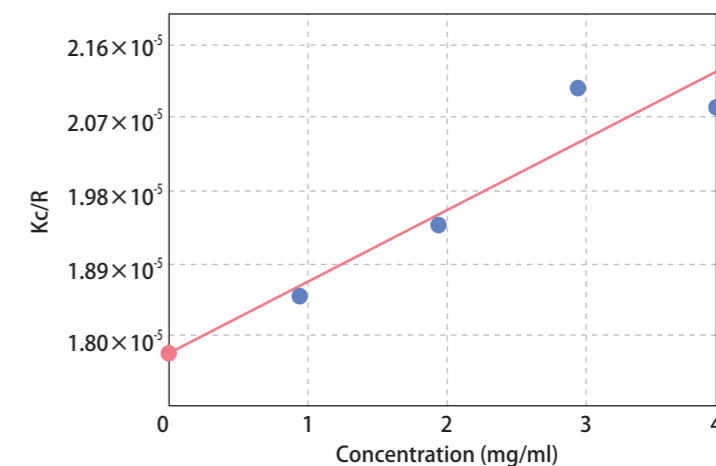


Fig. 1 Debye plot analysis for Tween 20

Table 1 Results for molecular weight measurement of Tween 20

Molecular weight	Second virial coefficient	Aggregation number	dn/dc
56110	4.35E-7 (cm ³ g ⁻² mol)	45	0.1256

15

ELSZ

Evaluating the properties of an electroconductive polymer (PEDOT/PSS)

Particle diameter

Purpose In recent years, electroconductive polymers have emerged as materials characterized by electroconductivity similar to metals. These materials have found applications in various fields of electronics and other industries. Polyethylene-sulfonic-acid-doped polyethylene dioxythiophene (PEDOT/PSS) is a representative electroconductive polymer. Due to small visible absorption, PEDOT/PSS is expected to replace ITO, a transparent electrode material.

We measured the particle diameters of two kinds of PEDOT/PSS of different compounding ratios.

Result Figures 1 and 2 show the particle size distributions for PEDOT/PSS of different compounding ratios. The average particle diameter of low conductive grade PEDOT/PSS of the higher PSS compounding ratio was 268.6 nm. The average particle diameter of conductive grade PEDOT/PSS of the lower PSS compounding ratio was 2,555.6 nm. We observed two peaks in the particle size distribution of each PEDOT/PSSs, suggesting the presence of aggregation. The higher hydrophilicity conferred by sulfonic acid is believed to result in smaller particle diameters as the PSS compounding ratio increases. PEDOT/PSS is known to present significant variations in physical properties depending on compounding ratio. We found that particle diameters also had significant effects.

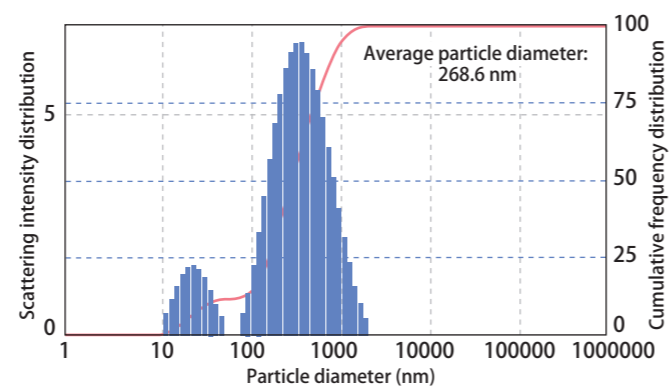


Fig. 1 Distribution of particle diameters of low conductive grade PEDOT/PSS

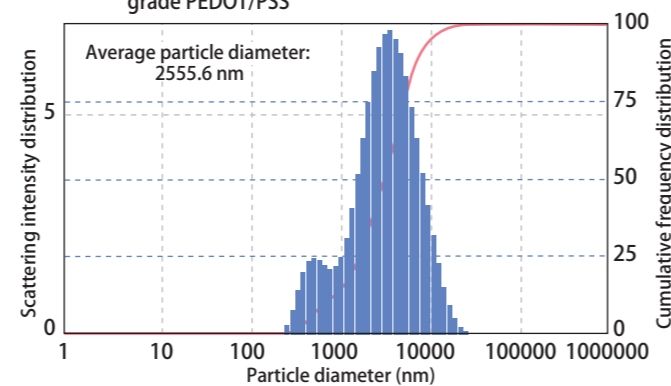


Fig. 2 Particle size distribution of conductive grade PEDOT/PSS

16

ELSZ

Evaluating the alternate lamination method based on solid surface potential

Zeta potential

Purpose Alternate lamination method (alternate adsorption method) is a method for forming thin films by adsorption induced by electrostatic interactions and the repeated alternate immersion of a substrate in a positive-ion-existing aqueous solution and a negative-ion-existing aqueous solution. Due to the promise of nano order thickness control, this method is expected to emerge as a next-generation film thickness coating method for LCDs, PDPs, semiconductors, and optics.

We measured the zeta potential of a layer of thin films formed on a slide glass substrate by the alternate lamination method using cationic and anionic polymer solutions. We used polyethyleneimine (PEI) as the cationic polymer. As the anionic polymer, we used Nafion with sulfone groups, which is also used as a polymer electrolyte film for fuel cells.

Result Figure 1 shows the zeta potentials of the respective layers when alternately laminating PEI and Nafion four times. In the lamination process, we confirmed the alternating inversion of electric charge. This indicates that the polymers are electrostatically adsorbed and confirms the alternate lamination of PEI and Nafion. Measuring solid surface potential is an effective method for evaluating the process of laminating substrates.

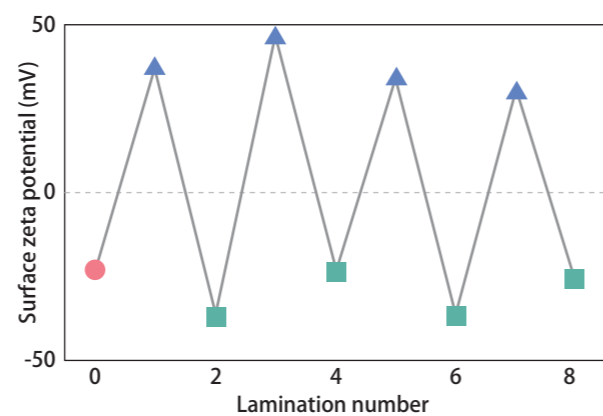


Fig. 1 Zeta potential of glass substrate to which PEI and Nafion were laminated four times in alternation

● : Surface potential of slide glass before immersion
▲ : Surface potential of slide glass immersed in PEI solution
■ : Surface potential of slide glass immersed in Nafion solution

17

ELSZ

Temperature gradient evaluation of polystyrene in cyclohexane

Particle diameter

Purpose Known to be a poor solvent of polymer polystyrene, solvent cyclohexane is known to be most effective at 34.5°C (θ temperature). We predicted that the proliferation of polymer chains would change as temperatures moved above or below temperature θ .

We used the ELSZ-2000ZS temperature gradient function to measure the dynamic light scattering of a cyclohexane solution of polystyrene (Mw = 422000; product of Toso) as well as the effects of changing temperatures on hydrodynamic diameter (2Rh).

Result We determined the hydrodynamic diameter at each polystyrene concentration (0.5, 1.0, 1.5, 2.0, 3.0 mg/ml) while changing temperatures in 0.5°C and 1°C decrements from 40°C to 30°C. Certain polymer solutions exhibit concentration dependence in aspects such as solution viscosity, depending on the structure of the polymer. Figure 1 shows a plot of temperature vs. extrapolated values to zero based on hydrodynamic diameters obtained at each concentration. The hydrodynamic diameter of polystyrene tends to increase as temperatures rise. The proliferation of polymer chains vary when temperatures rise or drop below the θ temperature.

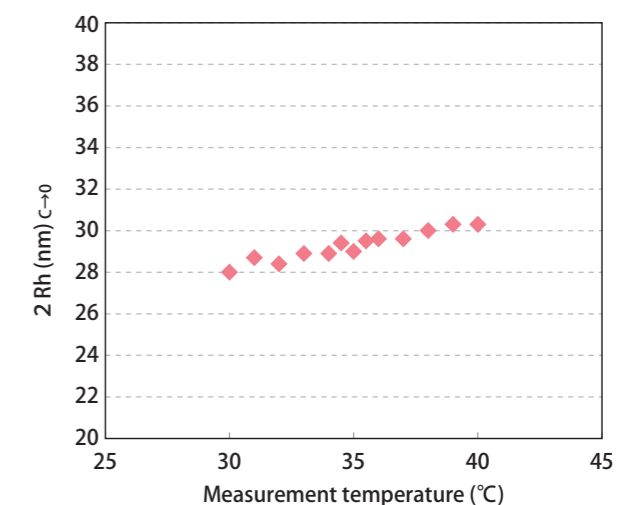


Fig. 1 Effects of changing temperature on the hydrodynamic diameter of polystyrene in cyclohexane

18

SLS

Evaluating the characteristics of functional polymers by static light scattering

Molecular weight

Purpose In recent years, in the pursuit of advanced functions, researchers have sought to modify the shape and structure of various polymers and to add various functional groups. One consequence has been that molecular weight measurements by size exclusion (GPC) no longer provide accurate molecular weights.

We evaluated the molecular weights of poly(methyl methacrylate) (PMMA) samples of near-identical molecular weight and different shapes by static light scattering.

Result The molecular weights of random PMMA and grafted PMMA as measured by static light scattering were quite similar: 157000 and 140000. However, when measured by the GPC method, the molecular weight of random PMMA was 150000 and grafted PMMA 70000, a near two-fold difference. This is because the GPC method relies on size exclusion, which is influenced by polymer density. In addition to molecular weight, static light scattering also gives the radius of gyration and the second virial coefficient, an index of affinity for the solvent.

The radii of gyration of the random and grafted PMMA were 252 Å and 115 Å, respectively. This difference is proportional to the difference in molecular weights obtained by the GPC method, demonstrating that the static light scattering method is a useful means for molecular weight measurements and for characterizing the radius of gyration and other characteristics of multi-functionalized polymers.

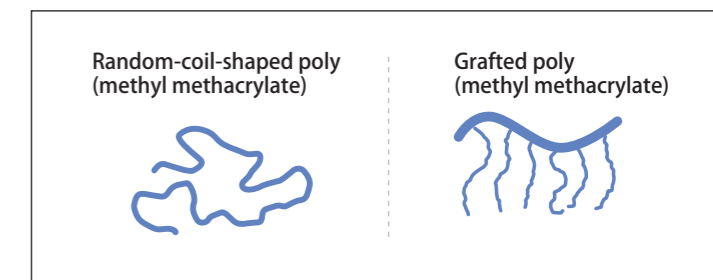


Fig. 1 Structures of random and grafted PMMA

Table 1 Results for molecular weight measurements of PMMA by static light scattering

Sample	Light scattering method				GPC method
	Molecular weight	Radius of gyration	Second virial coefficient	Solvent	
Random PMMA	157000	252	0.000451	THF	150000
Grafted PMMA	140000	115	0.000240	THF	70000

19 ELSZ Zeta potential evaluation for plastic containers

Particle diameter

Purpose Used in various industries in containers, packaging, electric appliances, automobiles, and pharmaceuticals, plastics are a staple of daily life. Compositions range from single materials to composites.

We measured the inner surface potential of various plastic containers: polyethylene (PE), polypropylene (PP), tetrafluoroethylene-perfluoroalkyl vinyl ether copolymer (PFA), and polyethylene terephthalate (PET).

Result Figure 1 shows pH titration results for the surface zeta potential of each container. The isoelectric points were found to be around pH4 for PE and PP. Fluorinated PFA was negatively charged in the range from pH3 to pH9 and lacked an isoelectric point. PET wasn't charged across the range of pH values. Since PET is known to be inherently negatively charged, the surface of the container was determined to have been treated.

Since surface potential depends on specific materials, potential interactions between the liquid to be placed in a container and the material itself must be considered.

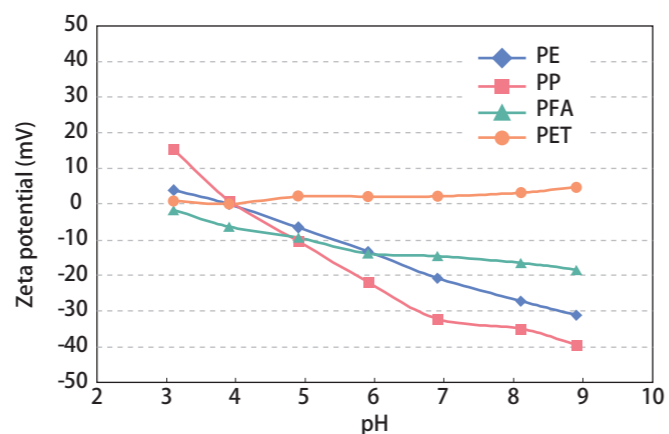


Fig. 1 Results for pH titration of each plastic container

20 CE Quantitative evaluation of impurities in terephthalic acid

Separation analysis

Purpose Terephthalic acid is used as a raw material for PET bottles used to distribute drinking water, for film, for fiber, and other materials. PET purity varies with specific applications. This requires analysis of not just terephthalic acid but byproducts. Byproducts may include benzoic acid, terephthalaldehyde acid, p-toluic acid, and so forth.

We performed an analysis to detect these byproducts in terephthalic acid.

Result Figure 1 shows the electropherogram of terephthalic acid (1.8 g/100 ml). Following the peak corresponding to terephthalic acid, the main component, we detected peaks corresponding to benzoic acid, terephthalaldehyde acid, and p-toluic acid. Separating the components took 12 minutes. Based on the peak area for each, the concentration of p-toluic acid was greatest.

This shows capillary electrophoresis is a fast and effective way to measure the purity of various substances and impurities.

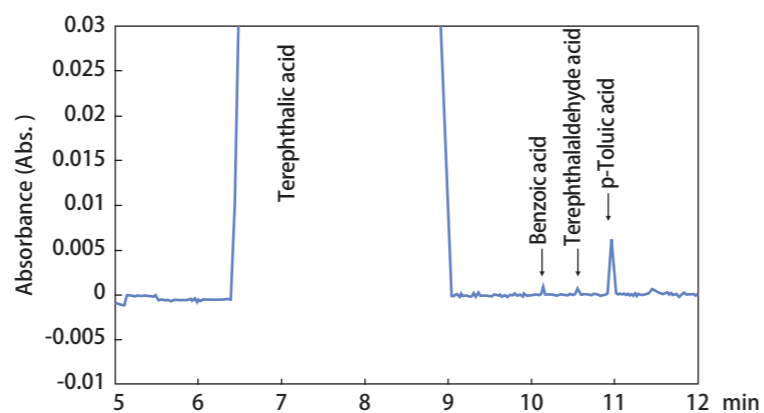


Fig. 1 Electropherogram of terephthalic acid
Capillary tube: inner diameter 75 μ m \times 80 cm
Electrophoresis liquid: α -HFH101

21 ELSZ Evaluating casein at normal and low temperatures

Particle diameter Zeta potential

Purpose Casein accounts for some 80% of all proteins in milk and plays important roles not just as a nutrient, but in processing. Rather than a single protein, casein consists of three main components: α -casein, β -casein, and κ -casein.

We dissolved casein in 50 mM Tris-HCl buffer solution (pH8) to a concentration of 1 mg/mL and performed measurements after filtration through a filter with pore size of 0.1 μ m.

Result Casein exists in the form of casein micelles ranging from 150 nm to 200 nm. Particle diameters at 4°C are somewhat larger than at 25°C, primarily because casein micelles are stabilized by hydrophobic bonding. Since hydrophobic bonds are weaker at lower temperatures, particle diameters will tend to increase as the structure of the micelles loosens.

A look at particle size distributions shows a shift to larger particles at lower temperatures. With respect to zeta potential, the negative charge at 4°C is somewhat lower than at 25°C. This is assumed to occur because β -casein, with its large negative charge, is isolated at lower temperatures, reducing the overall negative charge of the casein micelle and further reducing the interfacial potential.

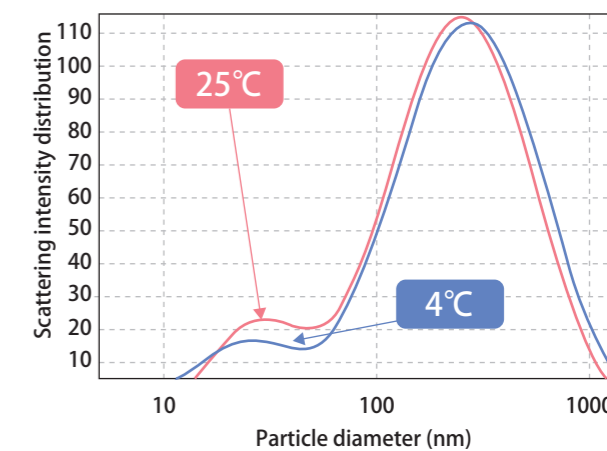


Fig. 1 Distribution of casein particle sizes

Table 1 Measurement results for the particle diameter and zeta potential of casein

Temperature ($^{\circ}$ C)	Average particle diameter (nm)	Zeta potential (mV)
25	157.6	-23.4
4	169.4	-18.4

22 ELSZ Evaluating fibrous and filamentous samples

Zeta potential

Purpose Zeta potential of fibrous substances is known to be closely related to the surface state of fibers and adsorption phenomena associated with various substances on the surface. The zeta potential of fibers has been evaluated by the flow potential method in research related to moisture absorption, swelling, dyeing, cleaning, and other applications. Previously, measurements of fibrous or filamentous samples by the electro-osmotic flow method posed difficulties because the samples tend to absorb water. The dedicated spacer shown in Figure 1 makes such measurements easier.

We mounted silk and cotton thread on a dedicated spacer and measured the zeta potential of each fiber in the acidic region from pH2.5 to pH5.8.

Result Figure 2 shows measurement results for the pH dependence of the fiber-surface zeta potential of silk and cotton thread. We observed differences in the isoelectric points of silk and cotton thread inherent to the materials themselves.

Since this method is capable of simultaneously obtaining not just the surface zeta potential of fibers but zeta potential of particles in solution, it has applications in the development of colloid dispersion particles for use as cleansers, softeners, and dyes.



Fig. 1 Filamentous sample set on spacer

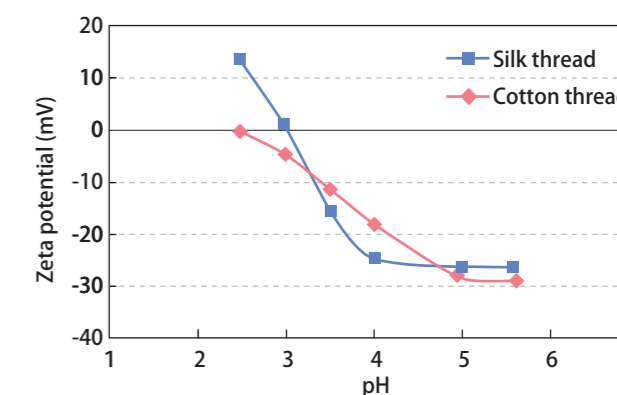


Fig. 2 Results for pH titration of surface zeta potential of silk and cotton thread

23

ELSZ Evaluating zeta potential in the fiber dyeing process

Zeta potential

Purpose Since silk thread is amphoteric and has acidic (carboxylic) groups and basic (amino) groups, the pH dependence of its surface zeta potential is known to have an isoelectric point around pH3. In the process of fiber dyeing, the process of dye adsorption to the fiber surface is said to be the key process governing. An electric double layer forms during the process; molecules forming the surface of the fibers dissociate, while dyes and other molecules in the liquid phase (dye bath phase) are adsorbed as ions. Thus, the zeta potential is believed to contribute significantly to the adsorption of dyes to fiber surfaces.

We measured the surface zeta potential of silk thread in the pH region (pH3 or below) in which the zeta potential of silk thread becomes positive. We added acidic dye (azo dye (orange II)) to silk thread in concentrations ranging from 0 to 1 mM.

Result Figure 1 shows the dye (orange II) addition concentration dependence of surface zeta potential of silk thread. As orange II concentrations increase, the surface zeta potential of silk thread changes sign from positive to negative, while the absolute value increases as well. It appears that the dye is adsorbed to the filament surface and the negative charge conferred by dye acidic groups (sulfone groups).

Measuring surface zeta potential is a useful method for investigating how well dyes will be absorbed by specific surface fibers.

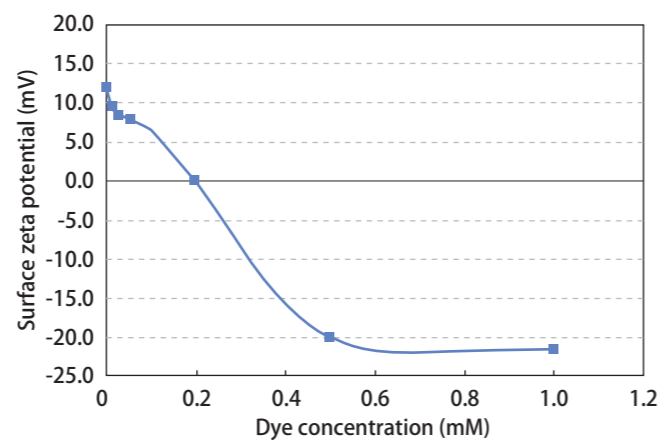


Fig. 1 Dye (orange II) concentration dependence of the surface zeta potential of silk thread

24

ELSZ Evaluating printer paper surfaces

Zeta potential

Purpose Inkjet printer paper comes with various coatings to improve ink fixation and coloring. As is generally known, when a solid surface and particles have opposing charges, electrostatic interactions result in the ready absorption of particles. Measuring the surface zeta potential of inkjet printer paper is useful in studies of the adsorptivity of ink (particles) on paper (solid surfaces).

We measured the surface zeta potential of four types of commercially available inkjet printer paper from the same manufacturer.

Result The surface zeta potentials for the paper samples were 0 mV for plain paper and photographic paper, negative for matte paper, and positive for glossy paper. Thus, the surface zeta potential of inkjet printer paper varies significantly by type. The difference appears attributable to paper coatings.

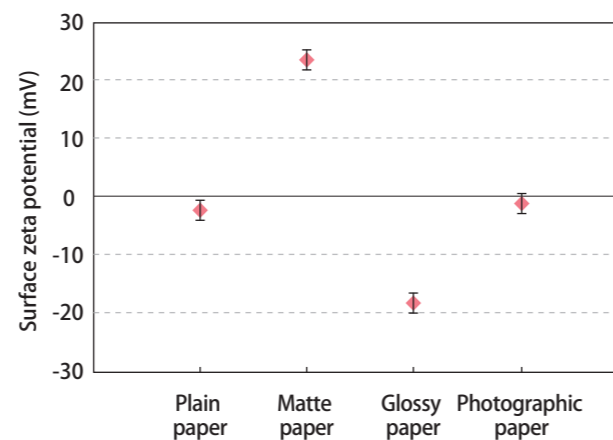


Fig. 1 Measurement results for zeta potential of surface of printer paper

memo

memo

memo